ENCIT 2018

17th Brazilian Congress of Thermal Sciences and Engineering
November 25th-28th, 2018, Águas de Lindóia, SP, Brazil

ENCIT-2018-0259
CFD ANALYSIS OF PRINTED CIRCUIT HEAT EXCHANGER (PCHE) FOR AIR-WATER

Ana Carolina Pereira de Oliveira
Nuclear Engineering Program — PEN/COPPE
Federal University of Rio de Janeiro — UFRJ, Rio de Janeiro, Brazil
acoliveira@nuclear.ufrj.br
Kelvin Chen
Mechanical Engineering Program — PEM/COPPE
Federal University of Rio de Janeiro - UFRJ , Rio de Janeiro, Brazil
kelvinchen89@gmail.com

Andre Sampaio Monteiro
Research Center — CENPES/PETROBRAS
Rio de Janeiro, Brazil
asmonteiro@petrobras.com.br

Carolina Palma Naveira Cotta
Mechanical Engineering Program — PEM/COPPE
Engineering of Nanotechnology Program — PENT/COPPE
Federal University of Rio de Janeiro — UFRJ , Rio de Janeiro, Brazil
carolina@mecanica.coppe.ufrj.br

Jian Su
Nuclear Engineering Program — PEN/COPPE
Engineering of Nanotechnology Program — PENT/COPPE
Federal University of Rio de Janeiro —- UFRJ , Rio de Janeiro, Brazil
sujian@nuclear.ufrj.br

Abstract. *Heat exchangers are used in a wide range of industrial operations. However, demands as space restriction and weight and greater efficiencies have made compact heat exchangers very popular. Printed circuit heat exchangers (PCHE) are a promising option due to their compactness and high performance. The present work aims to contribute with the proposition of the physical-mathematical modelling for the performance evaluation of the PCHE mini channels applied to industry operations. A Computational Fluid Dynamics analysis was performed considering a zigzag mini channels for air-waiter. The calculated temperature profiles were considered suitable for typical applications in offshore oil and gas production and the results for heat transfer were adequate for this type of application and new correlations for Nusselt number and friction factor were proposed.*

Keywords: *Compact heat exchangers, PCHE, zigzag mini channels, CFD*

1. INTRODUCTION

Heat exchangers are widely used in the industrial processes. In many cases, there are restrictions such as size and weight as well as high performance requirements, which lead to the development of new technologies for heat exchangers. The compact heat exchangers have a much higher heat exchange surface area density than the normal heat exchangers, as well as higher heat transfer coefficients (Southall *et al.*, 2008). Other advantages are high operating ranges of temperature and pressure and lower manufacturing costs. A disadvantage is the high pressure drop due to the clogging of the channels throughout the operation.

Printed Circuit Heat Exchanger (PCHE) is one of those technologies that shows promise due to its compactness and high performance. It was developed in the 1980s by Sydney University for refrigeration and was used for the oil and gas industry being developed by Heatric Company (Ma *et al.*, 2015). The PCHE is a plate type exchanger with the flow channels produced by photochemical etching on flat metal plates. Figure 1 shows a section trough a PCHE.

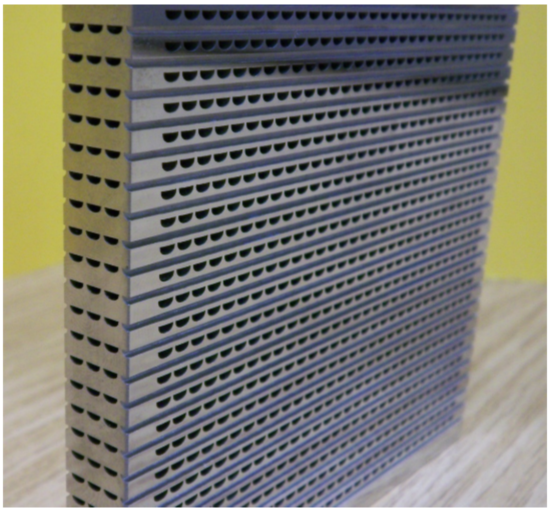

Figure 1. PCHE section (Southall *et al.*, 2008)

Kim *et al.* (2008) investigated heat transfer and pressure drop in PCHE with turbulent flow of supercritical CO_2-CO_2 as hot and cold fluid in semicircular zigzag channels to validate the physical-mathematical model and then proposed to change the geometry through of the airfoil-shaped fin insertion to optimize performance by reducing the pressure drop, which allowed the choice of the model for the present work. Kim *et al.* (2009) performed a CFD analysis with helium as hot and cold fluid to calculate the local Nusselt number of an experiment with a PCHE with semicircular zigzag channels arranged in the form of a hot and a cold channels interspersed and the present work used the same approach in the results analysis. VanAbel *et al.* (2011) carried out CFD simulations zigzag channel simulations of a PCHE with different turbulence models showing the efficiency of each one. Finally, Kim *et al.* (2016) performed a CFD analysis for the pressure drop and variation of the Nusselt number in a PCHE with supercritical CO_2 with turbulent flow in semicircular zigzag channels arranged in a cold channel between two hot channels, validating by comparing their results with experimental results and proposing new correlations for the Nusselt number and the friction factor, which was here considered as a main reference for the mathematical formulation although taking account the change regarding the working fluid.

The present work aims to provide some parametric analyses in the performance of a PCHE through a CFD simulation performed in the ANSYS platform. The obtained results will be compared with available correlations from the literature for Fanning factor and Nusselt numbers. The geometry here employed was based on the one studied by Kim *et al.* (2016) but using air-water pair to show the performance and the feasibility for other applications in industry and propose new correlations.

2. METHODOLOGY

The geometry construction, mesh generation, and computational simulation were carried out by using the software ANSYS v18.2. The mesh was generated by using ANSYS Design Modeler.

A transient simulation would take a long time and would have a high computational cost. Therefore, the simulations was performed using the pseudo transient under-relaxation method where a pseudo time step size is defined to control the under-relaxation, to avoid possible slow convergence on the steady state solution.

In this section, it will be shown the construction of the physical model, the parameters and properties used and the method of resolution of the proposed problem.

2.1 Geometry

The geometry of the PCHE studied here consists of several plates of cold zigzag channels between plates of hot zigzag channels and is based on an experimental analyses of the PCHE (Kim *et al.*, 2016). It is assumed that it will be sufficient to simulate only a single cold channel between two hot ones, considering periodic boundary conditions on the walls. Figure 2(a) shows the cross section of a PCHE, Fig. 2(b) shows the cross section of the modeled channels and Fig. 2(c) shows the zigzag channels and where the periodic boundary conditions will be applied. To limit computational time, the analysis was done only with six total pitches, which leads to a total channel straight length of 54 mm just as Kim *et al.* (2016) geometry, while the experimental PCHE has straight length of 896 mm (100 pitches). The analysis were performed for zigzag angles of $32.5°$ for both, hot and cold channels, which is shown in Fig. 3.

Kim *et al.* (2016) carried out a mesh convergence, which served as the basis for the mesh here generated. In this way, a mesh was constructed with 18 inflation layers for the boundary layer with $y+$ of approximately 1, as recommended for the turbulence model. The resulting mesh consists of 3767105 elements. The converged mesh used by Kim *et al.* (2016) has

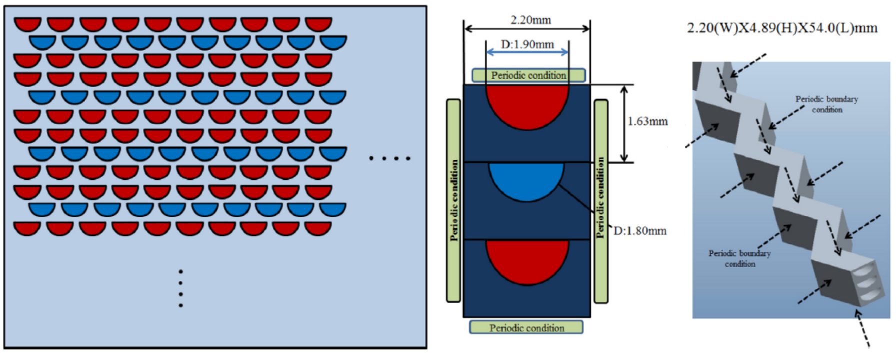

(a) Cross section of PCHE channels (b) Cross section of the channels studied (c) Modeled channels with periodic boundary conditions

Figure 2. PCHE channels (Kim *et al.*, 2016).

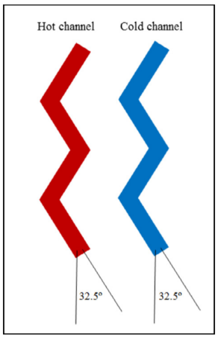

Figure 3. Angles of the channels (Kim *et al.*, 2016).

3772579 elements. Both meshes have similarities to the construction methods, boundary layer and quality, even though they have little difference in the number of elements.

2.2 Mathematical Formulation

We consider three-dimensional, pseudo-transient, uniform inlet velocity and conjugated heat transfer in a PCHE which are governed by the Navier-Stokes equations for the fluids and the energy equations for the fluids and for the solids, written as follows. All properties are considered constant.

$$\bigtriangledown \cdot \mathbf{u} = 0 \tag{1}$$

$$\rho_f \left(\nabla \cdot \mathbf{u} \right) = \nabla \cdot \left[-p\,\mathbf{I} + \mu_f (\nabla \mathbf{u} + (\nabla \mathbf{u})^{T_f}) \right] \tag{2}$$

$$\rho_f \, C_{p_f} (\mathbf{u} \cdot \nabla T_f) = \nabla \cdot (k_f \nabla T_f) \tag{3}$$

For the solid:

$$\nabla \cdot (k_s \, \nabla T_s) = 0 \tag{4}$$

where $\mathbf{u}$ is the fluid velocity, ρ_f the fluid density, C_{p_f} the fluid specific heat, p the fluid pressure, k_f the fluid thermal conductivity, T_f the fluid temperature, k_s the solid thermal conductivity, and T_s the solid temperature. Periodic boundary conditions were used on the surrounding walls.

The turbulence model used was the $k-\omega$ Shear Stress Transport (SST) and was chosen in accordance with Kim *et al.* (2016), being a good choice for this study. This model combines the formulas of the $k-\omega$ model in the regions near the walls with the equations of the $k-\epsilon$ model in the other regions. According to the VanAbel *et al.* (2011) study, the standard $k-\omega$ and $k-\epsilon$ models underestimate the drop in pressure although they have concordant heat transfer results. Therefore, the SST model becomes the best option for this analysis.

2.3 Test Cases

For the analysis with air and water, the properties were obtained on the NIST Chemistry WebBook platform and are summarized in Tab. 1 (Lemmon *et al.*, 2018). The Reynolds number, the inlet temperature and the pressure values were

Table 1. Properties of the model with Air-Water

	Hot Channel	Cold Channel
Fluid	Air	Water
Hydraulic diameter (mm)	1.1609	1.0998
Straight length (mm)	54	54
Inlet temperature (K)	333.15	298.15
Pressure (MPa)	1	0.1
Density (kg/m^3)	10.4736	997.05
Viscosity (Pa.s)	$2.0226 \cdot 10^{-5}$	$8.9008 \cdot 10^{-4}$
Heat capacity at constant pressure (J/kg.K)	1019.6	4181.3
Thermal conductivity (W/m.K)	0.029006	0.60719
Prandtl number	0.71097	6.12937
Reynolds number range	$2000 - 60000$	$200 - 6000$

based on the parameters of an experimental PCHE under study for water-air in turbulent flow in zigzag channels for a previous analysis of this flow.

Simulations were performed by varying the Reynolds number simultaneously in the hot and cold channels with a step of 10000 and 1000 respectively, for computational time savings and for the heat transfer to have a similar profile in each simulation. In each result the local and average Nusselt number and friction factor were analyzed, as well as the temperature at the outlet of the channels for the evaluation of the heat transfer.

3. RESULTS

For the Nusselt number and Fanning friction factor calculations, 35 planes were created perpendicular to the flow along the channel and equally spaced in 0.0015 m. The local Nusselt number was calculated by Eq. (5), where h_x is the average heat transfer coefficient at each plane, D_h is the channel hydraulic diameter and k_f is the fluid thermal conductivity. The channel averaged Nusselt number was calculate by arithmetic average of local values.

$$Nu_x = \frac{h_x \cdot D_h}{k_f} \tag{5}$$

The heat transfer coefficient was calculated by heat flux q'', bulk and wall temperature (T_b, T_w) of each plane (Eq. (6)). These variables were given by the software results.

$$h_x = \frac{{q_x}''}{(T_w - T_b)} \tag{6}$$

and q'' is calculated by Eq. (7), where T_f is the fluid temperature.

$$q'' = -k_f \left. \frac{\partial T_f(x)}{\partial y} \right|_{y_{axial}} \tag{7}$$

The Fanning friction factor was calculated by Eq. (8), where $P_{in} - P_x$ is the pressure drop at the plane x, ρ is the density, V_x is the velocity at the plane x and L_x is the active lenght from the inlet to the plane x.

$$f = \frac{(P_{in} - P_x)}{2\rho V_x^2} \left(\frac{D_h}{L_x} \right) \tag{8}$$

The results were compared with existing correlations for Nusselt number and friction factor. The correlations considered for Nusselt number with their respective validity ranges were: Dittus-Boelter (Eq. (9)), where L is the lenght of the channel, $n = 0.3$ for the fluid being cooled and $n = 0.4$ for the fluid being heated; and Gnielinski (Eq.(10)).

$$Nu = 0.023 Re^{0.8} Pr^n \qquad 0.6 \leq Pr \leq 160 \qquad Re \geq 10^5 \qquad L/D_h \geq 10 \tag{9}$$

$$Nu = \frac{(f/8)(Re - 1000)Pr}{1 + 12.7(f/8)^{1/2}(Pr^{2/3} - 1)} \qquad 0.5 \leq Pr \leq 2000 \qquad 3000 \leq Re \leq 5 \times 10^6 \tag{10}$$

For the Fanning friction factor, the correlations considered were Blasius (Eq. (11)) and McAdams (Eq.(12)) (Todreas and Kazimi, 2011).

$$f = \frac{0.316}{Re^{0.25}} \qquad 4000 < Re < 10^5 \tag{11}$$

$$f = \frac{0.184}{Re^{0.2}} \qquad 10^4 < Re < 10^6 \qquad (12)$$

Figure 4 shows the variation of the average outlet temperature with the Reynolds number at both hot and cold channels. Figure 5 shows the temperature distribution at outlet of the channels for Air-Water for each simulation with different Reynolds number.

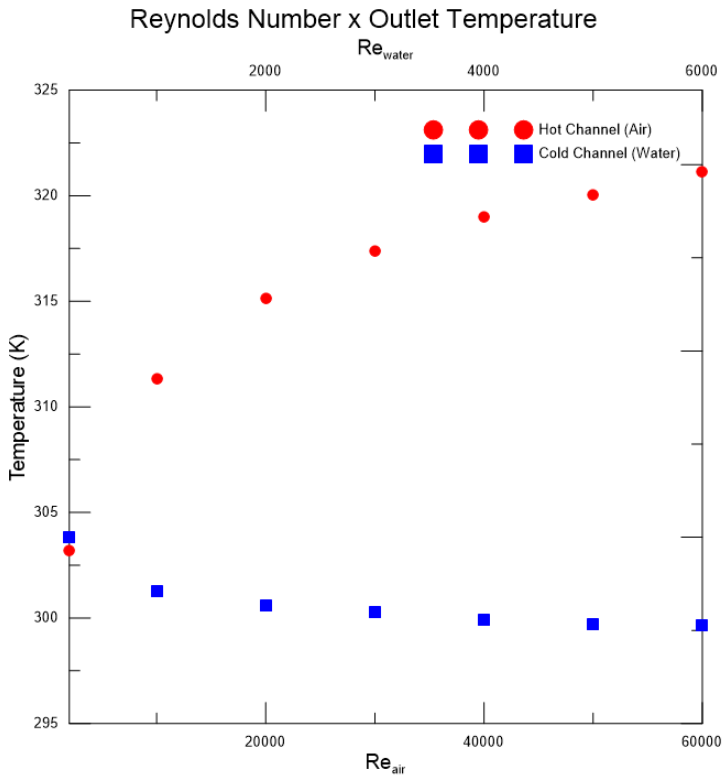

Figure 4. Average outlet temperature for hot and cold channels for Air-Water varying with Reynolds number

Figure 4 shows that as the Reynolds number increases, the difference between the outlet temperatures between the hot and cold channels increases, showing the influence of the flow velocity on the heat transfer.

From Fig. 5, it can be seen that the temperature of the air at outlet increases with the increase of the Reynolds number, illustrating this influence of the flow velocity on the heat transfer. For the water, the temperature varied very little for all the Reynolds numbers studied, but also decreases with the increase of the Reynolds number. This behavior is expected due to the increased velocity influencing the heat transfer. When the velocity increases, the temperature difference between the inlet and the outlet is lower.

It can also be seen that for low Reynolds numbers, hot spots appear on the walls near the exit of the cold channel. These hot spots disappear as the Reynolds number increases. This happens because the local heat transfer with smaller Reynolds numbers is larger due to the decrease of the boundary layer.

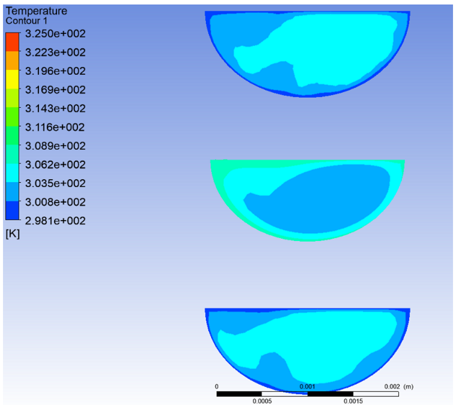

(a) Air $Re = 2000$; Water $Re = 200$

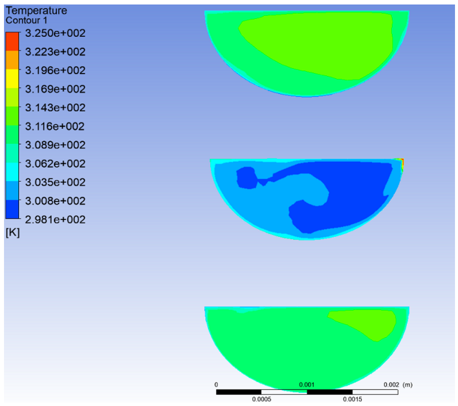

(b) Air $Re = 10000$; Water $Re = 1000$

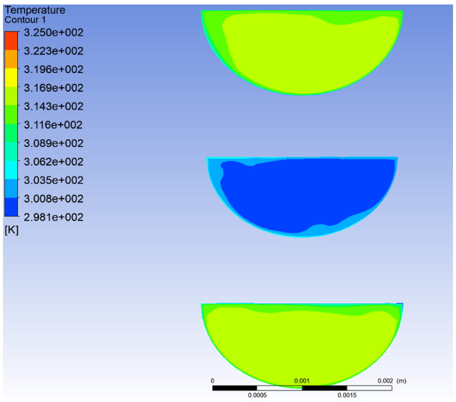

(c) Air $Re = 20000$; Water $Re = 2000$

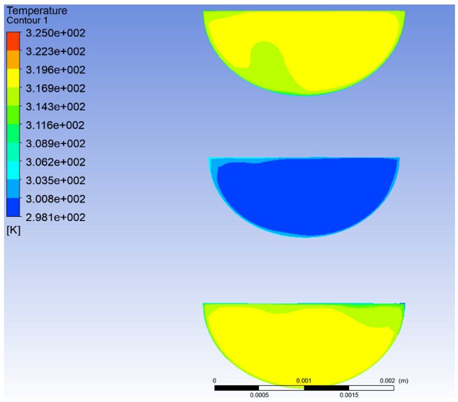

(d) Air $Re = 30000$; Water $Re = 3000$

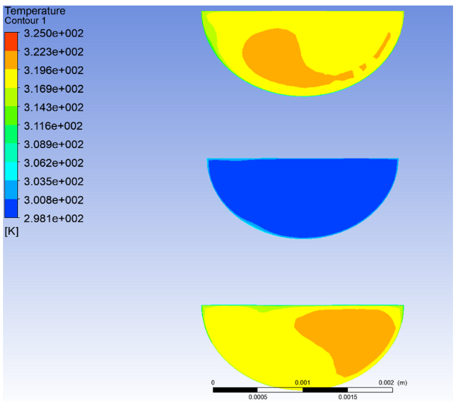

(e) Air $Re = 40000$; Water $Re = 4000$

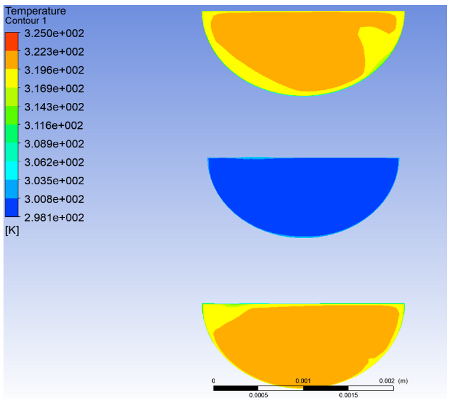

(f) Air $Re = 50000$; Water $Re = 5000$

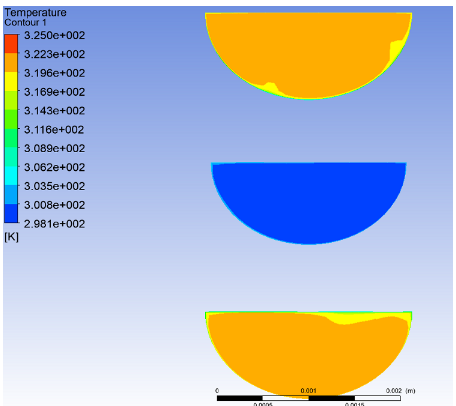

(g) Air $Re = 60000$; Water $Re = 6000$

Figure 5. Temperature distribution at outlet of hot and cold channels for different Reynolds numbers

Figure 6 shows the average Nusselt number and Fig. 7 shows the average Fanning friction factor for each Reynolds number, comparing with existing correlations.

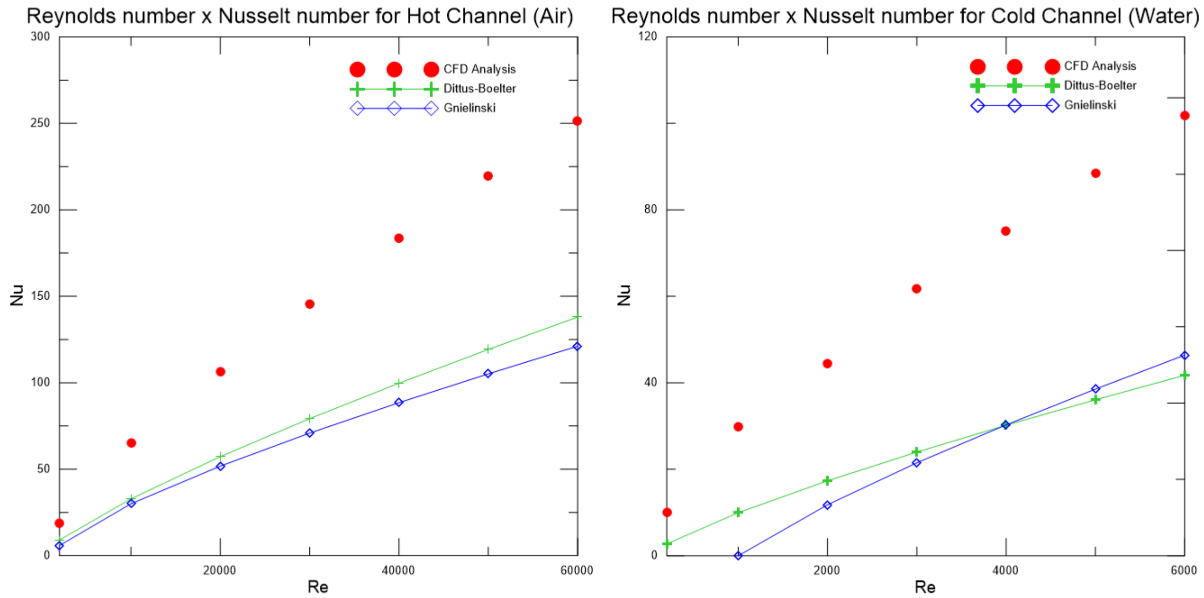

(a) Average Nusselt number for air channel (hot) (b) Average Nusselt number for water channel (cold)

Figure 6. Average Nusselt number for hot and cold channel for Air-Water

Looking at the results, the Nusselt numbers of the water are smaller than that of the air, even the water channel (cold) being between two air channels (hot). This happens because the Reynolds number values of the water are too high compared to the air Reynolds number, which causes the water heating by air to be lower than expected. This result is illustrated by the temperature distribution in Fig. 4, where it can be seen that the temperature of the water in the outlet varies very little. To achieve higher values of water temperature at the outlet, it is necessary to decrease the Reynolds number of the water, keeping the Reynolds number of the air.

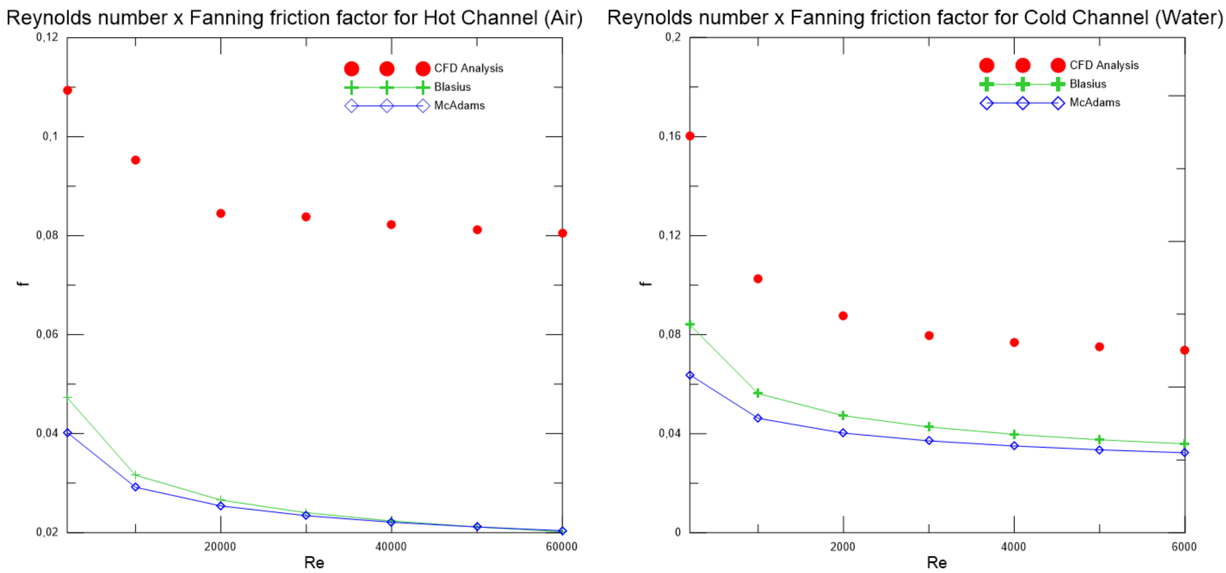

(a) Average friction factor for air channel (hot) (b) Average friction factor for water channel (cold)

Figure 7. Average Fanning friction factor for hot and cold channel for Air-Water

Based on these results profiles, it is possible to propose new correlations for Nusselt number and friction factor for this specific case of Air-Water in zigzag channels. For air, Eq. (13) is the correlation for Nusselt number and Eq. (14) is the correlation for friction factor for the air channel, with the respective standard errors and the coefficient of determination value (R^2). These correlations is valid for Reynolds number range between 2000 and 60000.

$$Nu = (0.05837 \pm 0.004709)Re^{(0.7601 \pm 0.008490)} \qquad R^2 = 0.9998 \tag{13}$$

$$f = (0.2224 \pm 0.01369) Re^{(-0.0939 \pm 0.006255)} \qquad R^2 = 0.9721 \tag{14}$$

For the water channel, Eq. (15) shows the correlation for Nusselt number and Eq.(16) shows the correlation for friction factor, with the respective standard errors and the coefficient of determination value (R^2). These correlations is valid for Reynolds number range between 200 and 6000.

$$Nu = (0.05893 \pm 0.007365) Re^{(0.6749 \pm 0,01682)} \qquad R^2 = 0.9988 \tag{15}$$

$$f = (0.8972 \pm 0.09581) Re^{(-0.2315 \pm 0.01036)} \qquad R^2 = 0.9834 \tag{16}$$

4. CONCLUSIONS

The calculated temperature profiles for air-water indicate that the PCHE studied is suitable for typical applications in offshore oil and gas production. In general, the heat transfer between water and air in a PCHE was efficient and feasible.

Experimental correlations should be developed in the future to allow the validation of the results obtained in the CFD analysis. For now, the CFD analysis allowed the verification of the three-channel model for air and water and it can be concluded that the PCHE is a good choice for this operation, noting that if the objective is, besides cooling the air, to heat the water, it would be necessary to work with a smaller Reynolds number range for water.

The Nusselt number and friction factor presented the same profile as that of the correlations but it is important to remember that the correlations of the literature were developed considering fluid flow in a straight channel. In zigzag channels the pressure drop is greater than in a straight channel, as well as better heat transfer, due to the changes of direction made by the flow. Thus, it is expected that the Nusselt number and friction factor will be higher for the zigzag channels compared to straight channels for the same Reynolds number value.

5. ACKNOWLEDGMENTS

The autors are grateful for the financial support provided by PETROBRAS S.A. and by Brazilian funding agencies: CNPq, FAPERJ and CAPES.

6. REFERENCES

Kim, D.E., Kim, M.H., Cha, J.E. and Kim, S.O., 2008. "Numerical investigation on thermal-hydraulic performance of new printed circuit heat exchanger model". *Nuclear Engineering and Design*, Vol. 238, pp. 3269–3276.

Kim, I.H., No, H.C., Lee, J.I. and Jeon, B.G., 2009. "Thermal hydraulic performance analysis of the printed circuit heat exchanger using a helium test facility and cfd simulations". *Nuclear Engineering and Design*, Vol. 239, pp. 2399–2408.

Kim, S.G., Lee, Y., Ahn, Y. and Lee, J.I., 2016. "Cfd aided approach to design printed circuit heat exchangers for supercritical co2 brayton cycle application". *Annals of Nuclear Energy*, Vol. 92, pp. 175–185.

Lemmon, E., McLinden, M. and Friend, D., 2018. *Thermophysical Properties of Fluid Systems*. NIST Chemistry Web-Book, NIST Standard Reference Database Number 69, Eds. P.J. Linstrom and W.G. Mallard, National Institute of Standards and Technology, Gaithersburg MD, 20899.

Ma, T., Li, T., Xu, X., Chen, Y. and Wang, Q., 2015. "Study on local thermal hydraulic performance and optimization of zigzag–type printed circuit heat exchanger at high temperature". *Energy Conversion and Management*, Vol. 104, pp. 55–66.

Southall, D., Pierres, L., R. and Dewson, S.J., 2008. "Design considerations for compact heat exchangers". In *Proceedings of ICAPP 2008*. Anaheim, CA, USA.

Todreas, N.E. and Kazimi, M.S., 2011. *Nuclear Systems Volume 1 Thermal Hydraulic Fundamentals*. CRC Press, Taylor And Francis Group, 6000 Broken Sound Parkway NW, Suite 300, Boca Raton FL 33487-2742, 2nd edition.

VanAbel, E.N., Anderson, M.H. and Corradini, M.L., 2011. "Numerical investigation of pressure drop and local heat transfer of supercritical co2 in printed circuit heat exchangers". In *Supercritical CO2 Power Cycle Symposium*. Boulder, Colorado, USA.

7. RESPONSIBILITY NOTICE

The authors are the only responsible for the printed material included in this paper.